One-neutron knockout from ^{57}Ni

K. L. Yurkewicz,[1,2,*] D. Bazin,[1] B. A. Brown,[1,2] J. Enders,[1,†] A. Gade,[1,2] T. Glasmacher,[1,2,‡] P. G. Hansen,[1,2]
V. Maddalena,[1,2,§] A. Navin,[1,‖] B. M. Sherrill,[1,2] and J. A. Tostevin[3]

[1]*National Superconducting Cyclotron Laboratory, Michigan State University, East Lansing, Michigan 48824, USA*
[2]*Department of Physics and Astronomy, Michigan State University, East Lansing, Michigan 48824, USA*
[3]*Department of Physics, School of Electronics and Physical Sciences, University of Surrey, Guildford, Surrey GU2 7XH, United Kingdom*
(Received 20 March 2006; published 16 August 2006)

The single-particle structure of ^{57}Ni and level structure of ^{56}Ni were investigated with the ^{9}Be $(^{57}$Ni,^{56}Ni$+\gamma)X$ reaction at 73 MeV/nucleon. An inclusive cross section of 41.4(12) mb was obtained for the reaction, compared to a theoretical prediction of 85.4 mb, hence only 48(2)% of the theoretical cross section is exhausted. This reduction in the observed spectroscopic strength is consistent with that found for lighter well-bound nuclei. One-neutron removal spectroscopic factors of 0.58(11) to the ground state and 3.7(2) to all excited states of ^{56}Ni were deduced.

I. INTRODUCTION

Doubly-magic nuclei are key benchmarks to our understanding of nuclear shell structure. Until experiments around ^{100}Sn become feasible, ^{56}Ni is the heaviest experimentally accessible doubly-magic nucleus in which protons and neutrons occupy the same orbitals. An early neutron-pickup experiment populating states in ^{57}Ni suggested that the low-lying excited states may not be purely single-particle in nature but may include contributions from ^{56}Ni excited states [1]. The β-decay of ^{57}Cu indicated [2] that the Gamov-Teller matrix element of its decay to the ground state of ^{57}Ni is significantly reduced compared to the single-particle value. Measurements of unusually high collectivity of ^{56}Ni [3–5] reinforced the questions about the single-particle character of the ground and lowest excited states of ^{57}Ni. The spectroscopic factors for the first three states of ^{57}Ni were measured in a (d, p) transfer reaction at low energy [6]. In contrast to the indications of collectivity from the measured ^{56}Ni $B(E2)$ excitation strength, the transfer experiment indicated that the first three states of ^{57}Ni are almost pure single-particle states.

Pickup and stripping reactions and extraction of spectroscopic factors can be used to resolve the nature of ^{56}Ni and the single-particle character of ^{57}Cu and ^{57}Ni. The accuracy of spectroscopic factors measured in this mass region via low-energy transfer reactions is limited by the lack of good optical model potential parameters. In experiments performed at high energies, analyses based on the sudden approximation and eikonal theory [7,8] are applicable and thus the model dependency is reduced. The corresponding experimental technique is one-nucleon knockout in inverse kinematics, a method which has been used to measure single-particle configurations over a range of nuclei since its development as a spectroscopic tool [9–13]. In this method, single-particle spectroscopy on the nucleus of interest is performed by extracting the following quantities: partial cross sections to ground and excited states of the knockout residues; the spectroscopic factors for the removal of a nucleon from a specific single-particle orbit of the projectile; and the orbital angular momentum of the removed nucleon. Measurements are performed in inverse kinematics at beam energies of greater than 50 MeV/nucleon.

In previous one-nucleon knockout experiments on well-bound nuclei, a reduction in measured spectroscopic strength with respect to shell-model predictions has been observed. The resulting reduction factor R_s, the ratio of experimental and theoretical spectroscopic strength, is 0.5–0.7 for one-proton and one-neutron knockout from stable ^{12}C and ^{16}O [14] and for one-neutron removal from well-bound $N = 16$ isotones [11] but closer to unity for one-proton knockout from the lighter weakly proton-bound nuclei ^{8}B, ^{9}C [15] and for the one-neutron knockout from the weakly neutron-bound ^{15}C to the ground state of ^{14}C [12]. Recently, a pronounced reduction of 0.24(4) has been observed in the one-neutron removal from ^{32}Ar [13], the most deeply-bound neutron system studied so far.

II. THEORETICAL ANALYSIS

In the technique of one-nucleon knockout, the measured cross sections are used to derive the one-nucleon removal spectroscopic factors via an extension of the eikonal model [8]. The cross section σ to a specific final state of the knockout residue (core) is related to the spectroscopic factor via

$$\sigma_{\text{exp}} = \sum_j C^2 S_{\text{exp}}(nlj)\sigma_{\text{sp}}(S_n, nlj), \tag{1}$$

$$\sigma_{\text{th}} = \sum_j \left(\frac{A}{A-1}\right)^N C^2 S_{\text{SM}}(nlj)\sigma_{\text{sp}}(S_n, nlj), \tag{2}$$

where the sum is taken over all non-vanishing nucleon-core configurations. The quantity C^2S is the spectroscopic factor for

the removal of a nucleon with given single-particle quantum numbers nlj. The factor $[(A/(A-1))^N]$ is a center-of-mass correction that has to be applied if spectroscopic factors are taken from shell model to obtain a theoretical cross section. In the center-of-mass correction, A is the mass number of the initial nucleus and N is the main harmonic oscillator quantum number associated with the relevant major shell [14]. The spectroscopic factor depends on the structure of the nucleus, whereas the single-particle cross section σ_{sp} comes from reaction theory, assuming unit single-particle strength.

The single-particle cross sections are highly dependent on the nucleon separation energy $S_{n,p}$ and the orbital angular momentum l of the removed nucleon. These were calculated in the eikonal model and include contributions from both the stripping and diffraction processes [8]. The removed-neutron wave functions in the ^{57}Ni ground state were calculated in Woods-Saxon potential wells with a diffuseness 0.7 fm. Their radius parameters were chosen so that the *rms* radius of each neutron orbital was consistent with those from a Skyrme SKX Hartree-Fock (HF) [16] calculation for ^{57}Ni when the depth of the Woods-Saxon potential was adjusted to reproduce the effective separation energy. The measured separation energy of $S_n = 10.247$ MeV [17] was used for the $p_{3/2}$ state and an effective separation energy of 14 MeV was estimated from the centroid of the $p_{3/2}f_{7/2}$ multiplet for the $f_{7/2}$ level. The orbital *rms* radii were assumed to be 4.14 and 4.17 fm for the $p_{3/2}$ and $f_{7/2}$ levels. The ^{56}Ni neutron and proton densities were also taken from HF, resulting in a *rms* matter radius of 3.64 fm for ^{56}Ni, consistent with ^{56}Fe. A Gaussian matter distribution was assumed for the ^{9}Be target with an *rms* matter radius of 2.36 fm.

Excited levels of ^{56}Ni and associated spectroscopic factors were calculated in the many-body shell model [18,19] using the FPD6 effective interaction [20]. For ^{57}Ni, the $\nu(f_{7/2})$ and $\pi(f_{7/2})$ closed shells plus one neutron in the $p_{3/2}$ orbit were assumed. For ^{56}Ni, calculations were performed with the $\nu(f_{7/2})$ and $\pi(f_{7/2})$ closed shells for the ground state, and for the excited states $\pi(f_{7/2})^8$ and $\nu(f_{7/2})^7$ with the $p_{3/2}$, $f_{5/2}$, and $p_{1/2}$ neutron shells active. In this approach, the spectroscopic factor for the removal of a neutron from the $p_{3/2}$ orbit leading to the ground state of ^{56}Ni is $C^2 S_{SM} = 1$ and the spectroscopic factors for removing a neutron from $f_{7/2}$ summed over all final excited states of ^{56}Ni ($T = 0$ and $T = 1$) is $C^2 S_{SM} = 8$. Considering the calculated energy levels of ^{56}Ni, we predict 7.36 of this to be below the proton separation energy.

The shape of the measured parallel momentum distribution of the ^{56}Ni residues is used to assign the orbital angular momentum for the removed nucleon. The theoretical parallel momentum distributions were calculated in a black-disk model [7], core-target collisions at small impact parameters (<7.2 fm) being assumed to result in fragmentation of the core. Interaction radii were chosen to reproduce the reaction cross sections of the free constituents.

III. EXPERIMENT AND DATA ANALYSIS

The experiment was performed at the National Superconducting Cyclotron Laboratory (NSCL). Acceleration of a beam of stable ^{58}Ni to an energy of 105 MeV/nucleon

and an intensity of 2 pnA was carried out in the K1200 cyclotron of the NSCL. The ^{58}Ni beam was incident on a 249 mg/cm^2 ^{9}Be production target. The A1200 fragment separator [21] was used to select a secondary beam of ^{57}Ni with an energy of 73 MeV/nucleon, an intensity of approximately 30,000 particles/s and a momentum spread of 0.5%. A 56.1 mg/cm^2 ^{9}Be target was located at the center of an array of 38 position-sensitive NaI(Tl) detectors [22] at the entrance to the S800 spectrograph [23]. Gamma rays were measured in coincidence with the knockout residues detected by the S800 focal-plane detector system [24]. The identification of the ^{56}Ni fragments was performed with energy loss and position information measured with the S800 spectrograph focal-plane detectors and using the time of flight taken between plastic scintillators at the exit of the A1200 fragment separator and the S800 focal plane (see Fig. 1).
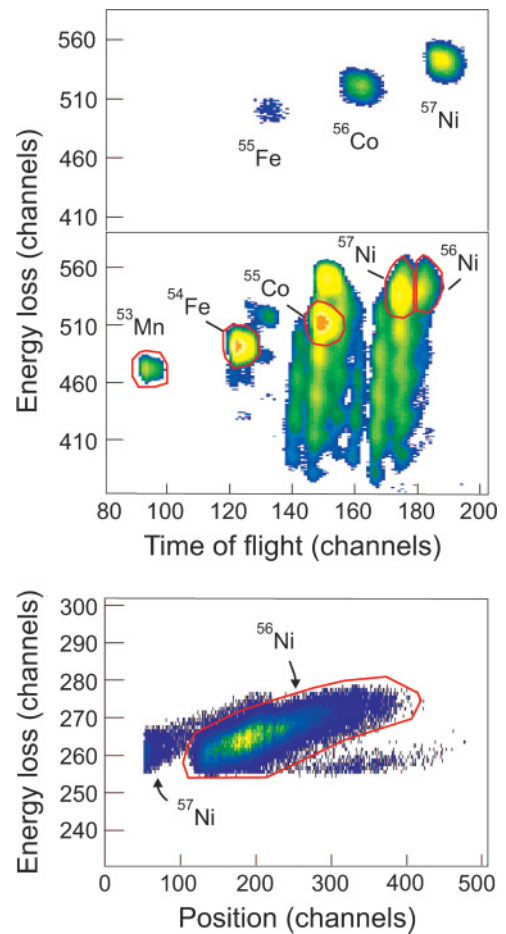

FIG. 1. (Color online) Particle identification in the S800 focal plane. The upper panel shows the energy loss measured in the ionization chamber versus the time of flight taken between two plastic scintillators for the unreacted beam (top) and the setting with the spectrograph centered on the one-neutron removal (bottom). The lower panel shows the correlation between the energy loss and the x-position (dispersive) in the focal plane. In this spectrum, a beam blocker had been inserted at the high-momentum side to block the tail of the unreacted ^{57}Ni beam. ^{56}Ni and ^{57}Ni isotopes can be clearly separated. The x-position relates to the parallel momentum.
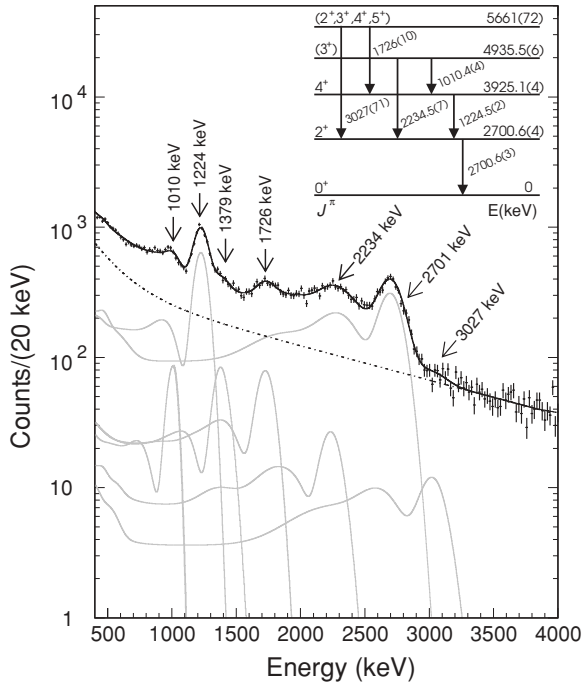
FIG. 2. Doppler-reconstructed ($\beta = 0.36$) projectile-frame γ-ray spectrum in coincidence with ^{56}Ni fragments detected in the spectrograph focal plane. The solid black line is the fit to the experimental spectrum containing the sum of the simulated response functions for seven γ-ray peaks (solid gray lines) and a double-exponential coincident background (dashed line), assumed to arise from excitations of the target. The inset shows a partial decay scheme for ^{56}Ni with a new proposed level at 5661(72) keV.

After the ^{56}Ni residues from one-neutron knockout were unambiguously identified, the coincident γ-ray spectrum was analyzed. Only the inner ring of 11 NaI(Tl) detectors [22] was used in this experiment. GEANT [25] simulations successfully modeled the γ-ray spectrum and the detector response. Simulations and experimental efficiencies measured with standard calibration sources agreed within 7.5%. The Doppler-reconstructed ($\beta = 0.36$) γ-ray spectrum in coincidence with ^{56}Ni fragments is shown in Fig. 2. The analytical curves, which were fitted to the simulated spectra and subsequently scaled to fit the experimental spectrum, can be seen as solid gray lines. The dashed line indicates the prompt, coincident background, described in this experiment by a double exponential curve. A similar background has been observed in previous knockout experiments [26–28], where it has been attributed to neutrons, γ rays, and charged particles interacting with the experimental apparatus and scintillators. The background determined for this experiment was 67% to 85% higher than that quoted for knockout on Si and S [29]. There may be evidence for an increase in coincident background with mass number or binding energy of the knocked-out nucleons.

IV. RESULTS AND DISCUSSION

A simplified level scheme including all γ-ray transitions observed in this experiment is shown in the inset of Fig. 2.

The placement of the 1726(10) and 3027(71) keV γ rays in coincidence with the 1224.5(7) and 2700.6(3) keV γ rays resulted in a level at 5661(72) keV. A 5668 keV level and associated 1744 keV de-excitation γ ray were observed in 1985 [30] and reported without uncertainty. Although an angular momentum assignment of $J^\pi = 6^+$ was proposed for the 5668 keV level, only $J^\pi = 2^+, 3^+, 4^+, 5^+$, are expected to be populated via the one-neutron knockout mechanism because of angular momentum considerations. No placement in the proposed level scheme was possible for the γ ray observed at 1379(10) keV.

The proton separation energy for ^{56}Ni [$S_p = 7.165(11)$ MeV] is significantly higher than the energy of the highest excited state observed in this experiment. Although excited states up to an energy of 7900 keV were predicted in a shell-model calculation, no higher-lying excited states could be identified experimentally above 5661 keV. Low statistics at high γ-ray energies contributed to the difficulty in resolving any transitions above 3100 keV. Therefore the branching ratios to the individual excited states of ^{56}Ni were not calculated because of the possibility of indirect feeding from higher-lying, unobserved excited states.

The parallel momentum distributions of the ^{56}Ni knockout residues were determined using the reconstructed scattering angle and fractional kinetic energy after the target, the momentum (20.26 GeV/c) and beam velocity $\beta = 0.36$ at the point of the γ-ray emission, and the mass of the fragments. Because of the complexity of the γ-ray spectrum of ^{56}Ni, it was not possible to isolate momentum distributions associated with individual final excited states. Instead, the momentum distributions associated with the knockout to all excited states and the ground state of ^{56}Ni were reconstructed from the measured momenta in coincidence and anti-coincidence with detected γ rays. The coincident (C) and anti-coincident (A) spectra shown in Fig. 3(a) and 3(b), respectively, can be written in terms of the momentum distributions to the ground state ($S_{g.s.}$) and all excited states (S_{exc}) of ^{56}Ni as

$$S_{exc}(p_\parallel) = \frac{1}{\epsilon}\left[C(p_\parallel) - \frac{\delta}{1-\delta}A(p_\parallel)\right]$$

$$S_{g.s.}(p_\parallel) = \left[1 + \frac{\delta}{\epsilon(1-\delta)}\right]\left[A(p_\parallel) - \frac{(1-\delta)(1-\epsilon)}{\epsilon+\delta-\epsilon\delta}C(p_\parallel)\right].$$

(3)

The average efficiency ε for the NaI(Tl) array is expected to be approximately 50% for an average γ-ray cascade of two, but was varied in the analysis to determine the best separation between $S_{g.s.}$ and S_{exc}. The probability that a γ ray not originating from the de-excitation of a knockout residue would be detected in coincidence with that fragment in the S800 focal plane is δ. For this experiment, a value of $\delta = 0.1$ was chosen, in agreement with previous experiments that determined a γ-ray background of 10% per fragment. The background appears to be higher in this experiment than the 10% assumed in experiments on lighter nuclei. However, with this choice of δ, a consistent separation of the ground state and excited state events was obtained with a choice of
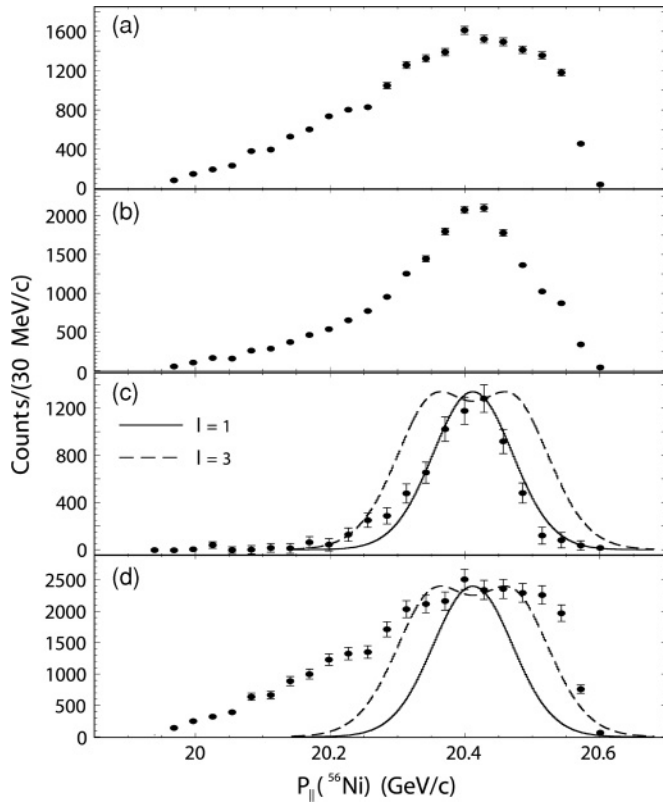
FIG. 3. Parallel momentum distributions associated with ^{56}Ni detected at the S800 focal plane. The distribution associated with ^{56}Ni fragments in coincidence with all γ rays between 250 and 7000 keV is shown in (a) and that associated with all remaining ^{56}Ni fragments in (b). The distribution associated with knockout to all excited states of ^{56}Ni is shown in (d) and that to the ground state in (c). The distributions in (c) and (d) were constructed assuming an average efficiency for the NaI(Tl) array of $\epsilon = 0.55$ and a background probability of $\delta = 0.1$ (see text for details).

$\epsilon = 0.55$. Thus the higher background used in the fit to the γ-ray spectrum in this experiment may be a result of multiple γ rays that could not be resolved because of the level density and low statistics at high energies. A 3.5% systematic error on the number of counts was included in the calculation of experimental cross sections because of the choice of the two parameters ϵ and δ. The resulting momentum distributions associated with the ground state and all excited states of ^{56}Ni are shown in Figs. 3(c) and 3(d). The errors shown include both statistical uncertainties and the systematic error from the choice of ϵ and δ. A similar analysis has been performed for the one-nucleon removal reactions on sd shell nuclei [31].

The shell model predicts that one-neutron removal to the ground state would be associated with an $l = 1$ distribution, because of the removal of the $1p_{3/2}$ valence neutron. Similarly, one-neutron removal to the excited states of ^{56}Ni would correspond to an $l = 3$ momentum distribution because of the orbital angular momentum carried by a neutron removed from the $0f_{7/2}$ shell. The ground state distribution shown in Fig. 3(c) is well described by an $l = 1$ theoretical curve centered at 20.42 GeV/c. The distribution associated with knockout to the excited states of the ^{56}Ni fragments, shown

in Fig. 3(d) is consistent with the theoretical curve for $l = 3$ with a low-momentum excess extending to approximately 20 GeV/c. This low-momentum tail as seen around 20.25 GeV/c in the excited-state momentum distribution [Fig. 3(d)] has been reported in several previous one-nucleon knockout experiments [26,29,32,33]. Tostevin [34] has shown that the asymmetric shape as observed for the knockout reactions on the halo nuclei ^{11}Be and ^{15}C can be reproduced by using a proper dynamical treatment of continuum-coupling effects in the diffractive channel of the knockout process. However, the same explanation is unlikely to hold for the well-bound ^{57}Ni. The present observation is very similar to the pronounced tail at low momentum reported in the one-neutron knockout from ^{46}Ar to the $7/2^-$ ground state of ^{45}Ar [33], where this asymmetry is discussed in the framework of deviations from eikonal theory.

The inclusive cross section σ_{incl} was calculated from the number of ^{56}Ni fragments detected in the spectrograph focal plane relative to the number of incident ^{57}Ni projectiles, normalized to the number of target nuclei. The inclusive cross section was calculated run by run, and the average for the three runs closest to the unreacted ^{57}Ni normalization run was used to determine $\sigma_{incl} = 41.4(12)$ mb. The partial cross sections to all excited states and the ground state of ^{56}Ni were determined using the same method as for the parallel momentum distributions. This resulted in branches of 81.3(35)% to all excited states and 18.7(35)% to the ground state, corresponding to a partial cross section to the ground state of 7.7(15) mb and to all excited states of 33.7(17) mb. The calculated stripping and diffraction components for the single-particle cross sections to the ground state and

TABLE I. Experimental cross sections (σ_{exp}) in mb and spectroscopic factors ($C^2 S_{exp} = \sigma_{exp}/\sigma_{sp}$) for the various final states of ^{56}Ni populated in the ^{9}Be(^{57}Ni,^{56}Ni+γ)X reaction at 73 MeV/nucleon. Theoretical single-particle cross sections ($\sigma_{sp} = \sigma_{str} + \sigma_{diff}$) were calculated in the eikonal model [7,8] for the stripping (σ_{str}) and diffractive (σ_{diff}) processes. Spectroscopic factors from shell model ($C^2 S_{SM}$) and the theoretical cross section σ_{th}, which combines the spectroscopic factors from the shell model and the single-particle cross section from the reaction theory following Eq. (2), are compared to the experimental values in terms of the ratio $R_s = \sigma_{exp}/\sigma_{th}$ (see text).

	Ground state	Excited states	Inclusive
I^π	0^+	2^+–5^+	
l	1	3	
σ_{str} (mb)	9.86	7.2	
σ_{diff} (mb)	3.48	2.0	
σ_{sp} (mb)	13.3	9.2	
σ_{exp} (mb)	7.7(15)	33.7(17)	41.4(12)
$C^2 S_{exp}$	0.58(11)	3.7(2)	
$C^2 S_{SM}$	1.0	7.36	
σ_{th} (mb)	14.0	71.4	85.4
R_s	0.55(11)	0.47(2)	0.48(2)

excited states of the fragments are listed in Table I, along with the total theoretical cross sections to both final states. The deduced spectroscopic factors were $C^2 S_{exp} = 0.58(11)$ for the ground state and $C^2 S_{exp} = 3.7(2)$ for all excited states.

The shell model is expected to most accurately predict the properties of nuclei at or near closed shells. As expected for ^{57}Ni, a semi-magic nucleus with only one neutron outside the doubly-magic $N = Z = 28$ core, the shell model correctly predicts the angular momentum of the knocked-out neutron for the ground-state configuration, shown by the good fit of the $l = 1$ shape to the momentum distribution associated with the ^{56}Ni ground state. Although the orbital angular momentum of knocked-out neutrons populating excited states of ^{56}Ni could not be well determined, a value of at least $l = 3$ should be assigned. The measured partial and inclusive cross sections, however, do not show good agreement with theory. The measured cross section to the ground state is 55(11)% of the theoretical ground-state cross section. The measured cross section to all excited states amounts to 47(2)% of the shell-model sum-rule theoretical cross section, and the inclusive cross section is 48(2)% of the theoretical inclusive cross section. The reduction in cross section translates into a reduction in measured spectroscopic strength relative to the shell model.

Several studies have been performed recently to explore this reduction in spectroscopic strength observed in one-nucleon removal experiments [11–15,33]. Proton removal from inelastic electron scattering has been considered the standard for the determination of absolute spectroscopic factors. It was shown that deduced spectroscopic factors from $(e, e' p)$ experiments for nuclei from mass 12 to 208 exhaust only about 60% of the single-particle shell model prediction [37–39]. Electron scattering data are available only for stable nuclei, and it is not possible to probe neutron occupancies within this approach. In contrast, the technique of one-nucleon knockout can be used to probe both proton and neutron occupancies in radioactive nuclei as well as stable species. It then becomes of interest to compare the spectroscopic factors deduced via one-proton knockout reactions to those from electron scattering. Brown *et al.* [14] compared theoretical cross sections calculated in the eikonal model with experimental cross sections from a series of one-nucleon knockout experiments. To facilitate a comparison between experiments, the reduction factor R_s was defined as the ratio between the experimental and theoretical cross sections. One-proton knockout on the stable nuclei ^{12}C and ^{16}O resulted in R_s values of 0.53(2) and 0.68(4), in agreement with the reduction factors deduced from the electron scattering experiments. One-neutron knockout from the same two stable nuclei yielded R_s values of 0.49(2) and 0.56(3), suggesting that one-neutron knockout experiments measure the same quantity as one-proton knockout and thus can also be used to measure absolute spectroscopic factors. The reduction in single-particle strength observed in the case of the radioactive nucleus ^{57}Ni is comparable to the reductions obtained for the single-neutron knockout of the two stable nuclei ^{12}C and ^{16}O [14] (see Fig. 4), consistent with the reduction observed in the one-neutron knockout on well-bound $N = 16$ isotones [11] and agrees with the quenching of single-particle strengths
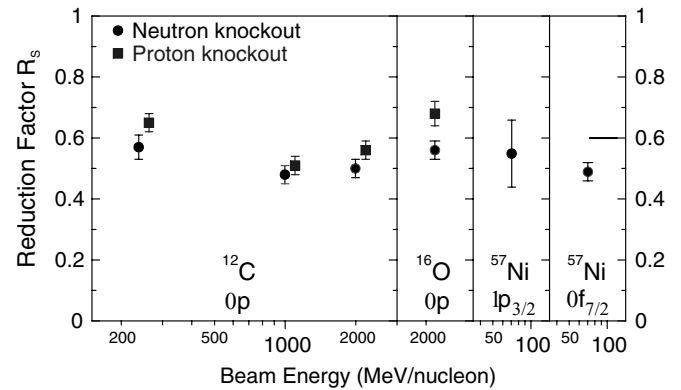

FIG. 4. Reduction factor R_s versus incident beam energy for one-nucleon knockout from the well-bound nuclei ^{12}C, ^{16}O, and ^{57}Ni. The circles (squares) indicate results from one-neutron (proton) knockout. R_s values for ^{12}C and ^{16}O were calculated in Ref. [14] from measurements performed at the Lawrence Berkeley National Laboratory [35,36].

observed for stable nuclei in electron scattering experiments [37–39].

It is suggested [13,15,37,39] that correlation effects (short-range, long-range, and tensor nucleon-nucleon interactions) that are absent from or only approximately treated in effective-interaction theory may explain some of the observed reduction in spectroscopic strength. Those correlations result in physical nucleon occupancies being reduced and spectroscopic strength shifted to higher energies; see Refs. [37,39]. For example, the repulsive short-range part of the interaction becomes important at distances of less than 0.4 fm and leads to high-momentum components in the nucleon wave function [37]. The importance of the coupling to surface phonons and giant resonances as contribution to the reduction has been discussed in Ref. [39].

In summary, spectroscopic factors for one-neutron removal from ^{57}Ni to the ground and all observed excited states of ^{56}Ni have been measured at 73 MeV/nucleon. The $l = 1$ character of the ^{57}Ni ground state and the $l = 3$ character of the first few excited states have been confirmed. The level scheme of ^{56}Ni was extended to include a level at 5661(72) keV, with two de-excitation γ rays. Finally, the phenomenon of a reduction in the measured spectroscopic strengths, as compared to shell-model predictions, has been confirmed in the exotic, doubly-magic ^{56}Ni—the heaviest nucleus yet measured via one-nucleon knockout. The observed inclusive cross section for knockout to ^{56}Ni was 48(2)% of the predicted shell-model value, in agreement with the reductions typically observed in stable, well-bound nuclei.

[1] C. R. Gould, D. P. Balamuth, P. F. Hinrichsen, and R. W. Zurmühle, Phys. Rev. **188**, 1792 (1969).

[2] T. Shinozuka, M. Fujioka, H. Miyatake, M. Yoshii, H. Hama, and T. Kamiya, Phys. Rev. C **30**, R2111 (1984).

[3] G. Kraus *et al.*, Phys. Rev. Lett. **73**, 1773 (1994).

[4] Y. Yanagisawa *et al.*, AIP Conf. Proc. **455**, 610 (1998).

[5] K. L. Yurkewicz *et al.*, Phys. Rev. C **70**, 064321 (2004).

[6] K. E. Rehm *et al.*, Phys. Rev. Lett. **80**, 676 (1998).

[7] P. G. Hansen, Phys. Rev. Lett. **77**, 1016 (1996).

[8] J. A. Tostevin, J. Phys. G **25**, 735 (1999).

[9] P. G. Hansen and B. M. Sherrill, Nucl. Phys. **A693**, 133 (2001).

[10] P. G. Hansen and J. A. Tostevin, Annu. Rev. Nucl. Part. Sci. **53**, 219 (2003).

[11] A. Gade *et al.*, Phys. Rev. C **69**, 034311 (2004).

[12] J. R. Terry, D. Bazin, B. A. Brown, J. Enders, T. Glasmacher, P. G. Hansen, B. M. Sherrill, and J. A. Tostevin, Phys. Rev. C **69**, 054306 (2004).

[13] A. Gade *et al.*, Phys. Rev. Lett. **93**, 042501 (2004).

[14] B. A. Brown, P. G. Hansen, B. M. Sherrill, and J. A. Tostevin, Phys. Rev. C **65**, 061601(R) (2002).

[15] J. Enders *et al.*, Phys. Rev. C **67**, 064301 (2003).

[16] B. A. Brown, Phys. Rev. C **58**, 220 (1998).

[17] M. R. Bhat, Nucl. Data Sheets **85**, 415 (1998).

[18] B. A. Brown and B. H. Wildenthal, Annu. Rev. Nucl. Part. Sci. **38**, 29 (1988).

[19] E. K. Warburton and B. A. Brown, Phys. Rev. C **46**, 923 (1992).

[20] D. R. Semon *et al.*, Phys. Rev. C **53**, 96 (1996).

[21] B. M. Sherrill, Nucl. Instrum. Methods B **70**, 298 (1992).

[22] H. Scheit, T. Glasmacher, R. W. Ibbotson, and P. G. Thirolf, Nucl. Instrum. Methods A **422**, 124 (1999).

[23] D. Bazin *et al.*, Nucl. Instrum. Methods B **204**, 629 (2003).

[24] J. Yurkon, D. Bazin, W. Benenson, D. J. Morrissey, B. M. Sherrill, D. Swan, and R. Swanson, Nucl. Instrum. Methods A **422**, 291 (1999).

[25] GEANT, Technical Report, W5013, CERN (1994).

[26] T. Aumann *et al.*, Phys. Rev. Lett. **84**, 35 (2000).

[27] V. Maddalena, Ph.D. thesis, Michigan State University (2000).

[28] V. Maddalena *et al.*, Phys. Rev. C **63**, 024613 (2001).

[29] J. Enders *et al.*, Phys. Rev. C **65**, 034318 (2002).

[30] J. Blomqvist *et al.*, Z. Phys. A **322**, 169 (1985).

[31] A. Navin *et al.*, Phys. Rev. Lett. **81**, 5089 (1998).

[32] V. Maddalena *et al.*, Nucl. Phys. **A682**, 332c (2001).

[33] A. Gade *et al.*, Phys. Rev. C **71**, 051301(R) (2005).

[34] J. A. Tostevin, Nucl. Phys. **A682**, 320c (2001).

[35] J. M. Kidd, P. J. Lindstrom, H. J. Crawford, and G. Woods, Phys. Rev. C **37**, 2613 (1988).

[36] D. L. Olson, B. L. Berman, D. E. Greiner, H. H. Heckman, P. J. Lindstrom, and H. J. Crawford, Phys. Rev. C **28**, 1602 (1983).

[37] V. R. Pandharipande, I. Sick, and P. K. A. deWitt Huberts, Rev. Mod. Phys. **69**, 981 (1997).

[38] G. J. Kramer, H. P. Blok, and L. Lapikś, Nucl. Phys. **A679**, 267 (2001).

[39] W. D. Dickhoff and C. Barbieri, Prog. Part. Nucl. Phys. **52**, 377 (2004).